NeuroImage 251 (2022) 118990

Contents lists available at ScienceDirect

NeuroImage

journal homepage: www.elsevier.com/locate/neuroimage

The oscillatory effects of rhythmic median nerve stimulation

Mairi S. Houlgreave[a,b,*], Barbara Morera Maiquez[a], Matthew J. Brookes[b], Stephen R. Jackson[a,c]

[a] School of Psychology, University of Nottingham, University Park, Nottingham NG7 2RD, UK
[b] School of Physics and Astronomy, Sir Peter Mansfield Imaging Centre, University of Nottingham, University Park, Nottingham NG7 2RD, UK
[c] School of Medicine, Institute of Mental Health, University of Nottingham, University Park, Nottingham NG7 2RD, UK

ARTICLE INFO

Keywords:
Magnetoencephalography
Median nerve stimulation
Mu
Beta
Entrainment
Steady-state evoked potentials

ABSTRACT

Entrainment of brain oscillations can be achieved using rhythmic non-invasive brain stimulation, and stimulation of the motor cortex at a frequency associated with sensorimotor inhibition can impair motor responses. Despite the potential for therapeutic application, these techniques do not lend themselves to use outside of a clinical setting. Here, the aim was to investigate whether rhythmic median nerve stimulation (MNS) could be used to entrain oscillations related to sensorimotor inhibition. MEG data were recorded from 20 participants during 400 trials, where for each trial 10 pulses of MNS were delivered either rhythmically or arrhythmically at 12 or 20 Hz. Our results demonstrate a frequency specific increase in relative amplitude in the contralateral somatosensory cortex during rhythmic but not arrhythmic stimulation. This was coupled with an increase in inter-trial phase coherence at the same frequency, suggesting that the oscillations synchronised with the pulses of MNS. The results show that 12 and 20 Hz rhythmic peripheral nerve stimulation can produce entrainment. Rhythmic MNS resulted in synchronous firing of neuronal populations within the contralateral somatosensory cortex meaning these neurons were engaged in processing of the afferent input. Therefore, MNS could prove therapeutically useful in disorders associated with hyperexcitability within the sensorimotor cortices.

1. Introduction

Neural oscillations are rhythmic variations in electrical activity which arise from the summation of synchronous postsynaptic potentials. Oscillations are categorised based on their frequency, with the alpha/mu-alpha (8–12 Hz) and beta (13–30 Hz) frequency bands being of particular importance when researching sensorimotor systems. In the contralateral sensorimotor cortex, oscillations in the 8–30 Hz range are suppressed during movement and movement preparation, but following movement there is a beta rebound, meaning their amplitude is briefly higher than at rest (Jurkiewicz et al., 2006; Pfurtscheller et al., 1996). Corticospinal excitability is known to be increased when sensorimotor oscillations are suppressed and reduced during the post-movement beta rebound (Chen et al., 1998). Higher beta activity has also been associated with a slowing of newly initiated movements (Gilbertson et al., 2005). Therefore, beta synchrony is frequently thought of as a mechanism which promotes maintenance of the current motor set (Engel and Fries, 2010). However, a newer theory suggests that beta is a marker of motor readiness, whereby a low level of beta activity indicates a higher likelihood that a movement will be generated (Jenkinson and Brown, 2011). In a study investigating the roles of alpha and beta oscillations through a novel saccade task a small positive correlation was found between saccade reaction time and contralateral sensorimotor beta power suggesting a role in somatosensory gating (Buchholz et al., 2014). On the other hand, alpha (mu-alpha in the sensorimotor cortex) synchrony has been linked to the inhibition of task irrelevant areas (Brinkman et al., 2014, 2016; Buchholz et al., 2014; Jensen and Mazaheri, 2010), with the network of regions involved in a task showing a desynchronisation of alpha oscillations (Haegens et al., 2010) and task-irrelevant regions showing an increase in alpha power (Brinkman et al., 2014; Buchholz et al., 2014). Various non-invasive brain stimulation (NIBS) techniques have been shown to modulate these oscillatory

Abbreviations: AAL, automated anatomical labelling; APB, abductor pollicis brevis; EMD, empirical mode decomposition; EMG, electromyography; FDR, false discovery rate; FLIRT, FMRIB's Linear Image Registration Tool; HT, Hilbert transform; IMFs, intrinsic mode functions; ISI, inter-stimulus interval; ITPC, inter-trial phase coherence; LCMV, linear-constraint minimum-variance; MEPs, motor evoked potential; MNI, montreal neurological institute; MNS, median nerve stimulation; NIBS, non-invasive brain stimulation; SEP, sensory evoked potential; SMA, supplementary motor area; SSEP, steady-state evoked potential; tACS, transcranial alternating current stimulation; TMS, transcranial magnetic stimulation.

* Corresponding author at: School of Psychology, University of Nottingham, University Park, Nottingham NG7 2RD, UK.
E-mail address: mairi.houlgreave@nottingham.ac.uk (M.S. Houlgreave).

https://doi.org/10.1016/j.neuroimage.2022.118990.
Received 26 December 2021; Accepted 10 February 2022
Available online 11 February 2022.

rhythms as well as behaviour (Joundi et al., 2012; Pogosyan et al., 2009; Thut et al., 2011b). As a result, there is widespread interest in the use of these techniques as potential forms of therapy in a multitude of disorders.

An interesting avenue for therapy using NIBS is entrainment; the process though which neuronal assemblies become synchronised to a rhythmic stimulus train (Thut et al., 2011a). Entrainment of oscillations in the 8–30 Hz range could prove therapeutically beneficial in patients with disorders characterised by sensorimotor hyperexcitability (Morera Maiquez et al., 2020b). Therefore, it is of interest that repetitive transcranial alternating current stimulation (tACS) at a frequency associated with periods of decreased corticospinal excitability can lead to a reduction in the velocity of movement (Pogosyan et al., 2009). In 2011, Thut and colleagues showed that rhythmic transcranial magnetic stimulation (TMS) of a parietal site at an individual's preferred alpha frequency caused region specific entrainment of brain oscillations (Thut et al., 2011b). These findings were specific to rhythmic TMS and were not seen with arrhythmic or sham stimulation control conditions. Given that tACS can have similar oscillatory effects it is interesting that application of a topical anaesthetic can significantly reduce entrainment, suggesting that the effects of tACS may be due to stimulation of the somatosensory cortex via peripheral nerves rather than direct stimulation of the cortex itself (Asamoah et al., 2019). Stimulation was applied at the tremor frequency of healthy volunteers (~8.70 Hz), resulting in increasing tremor entrainment with increasing tACS amplitude. However, when a topical anaesthetic was applied to the scalp this significant increase in phase locking to the stimulation with increasing tACS amplitude was not seen. While there was still a trend for this effect the authors argue that this is more likely to be caused by an incomplete block of the peripheral nerves rather than a transcranial mechanism being involved. This suggests that there is potential for the entrainment effects seen with tACS to be replicated through rhythmic stimulation of peripheral nerves rather than the cortex. In fact, rhythmic median nerve stimulation (MNS) at 12 Hz and 19 Hz (preprint) has been shown to cause a frequency specific increase in EEG power and inter-trial phase coherence (ITPC) over the contralateral sensorimotor cortex in healthy participants, which is not seen with arrhythmic stimulation (Morera Maiquez et al., 2020b, 2020a (preprint)). This suggests that rhythmic MNS may be able to entrain the sensorimotor cortex. Furthermore, when compared with no stimulation, delivery of 10 Hz rhythmic MNS has been shown to reduce the frequency of tics in Tourette syndrome patients, a disorder associated with sensorimotor hyperexcitability (Morera Maiquez et al., 2020b). These are important findings as, unlike tACS and TMS, MNS is portable, cheaper and requires little training, making it an ideal technique to be used therapeutically outside of the clinic. An ideal therapeutic intervention would induce long-term clinically beneficial aftereffects. It has been shown that oscillatory aftereffects following entrainment protocols are prevalent (Veniero et al., 2015). However, these aftereffects are not necessarily localised to the entrained frequency and have been inconsistent between experiments stimulating using the same frequency (Veniero et al., 2015). As such, more work is needed to understand the potential therapeutic uses of rhythmic brain stimulation as well as the possible entrainment of brain oscillations and their aftereffects.

When a sensory stimulus (such as MNS) is delivered a transient, phase-locked electrical potential can be recorded over the sensorimotor cortex which is known as a sensory evoked potential (SEP) (Vialatte et al., 2010). When longer trains of rhythmic stimuli are delivered, we can record steady-state evoked potentials (SSEPs) which appear as a sustained response at the frequency of stimulation (Regan, 1989, as cited in Vialatte et al. 2010, Regan, 1966). SSEPs are thought to either arise due to entrainment of a population of neurons (Herrmann, 2001) or due to linear superposition of SEPs in response to each pulse of the train (Capilla et al., 2011). Critically, both explanations could explain the increase in EEG/MEG power and ITPC at the frequency of stimulation (Capilla et al., 2011; Keitel et al., 2014). When refractoriness is taken into account there is compelling evidence for the superposition hypothesis (Capilla et al., 2011; Colon et al., 2012). Nevertheless, there is reason to believe both mechanisms coexist (Colon et al., 2012; Notbohm et al., 2016). Oscillating systems have a preferred frequency and when matched by the external stimulus train the system resonates (Colon et al., 2012; Herrmann, 2001; Notbohm et al., 2016; Vialatte et al., 2010). Therefore, at certain frequencies the signal recorded could be largely because of entrainment rather than rhythmic SEPs (Colon et al., 2012). Hence, in our study we delivered trains of MNS at 12 and 20 Hz during concurrent MEG recording to investigate entrainment effects (adapted from Morera Maiquez et al. 2020b). There is evidence that stimulation at these frequencies can cause a slowing of voluntary movement. Reaction times during correct responses of a choice reaction time task were slowed by rhythmic 12 Hz MNS (Morera Maiquez et al., 2020b), while 20 Hz tACS has been shown to slow the initial and peak velocity of a movement (Pogosyan et al., 2009) as well as reduce the initial and peak force rate of movements (Joundi et al., 2012). As both entrainment and SSEPs would cause populations of neurons within the sensorimotor cortex to fire synchronously we would expect no difference in the online behavioural effects of these interventions. However, entrainment may make it easier to elicit long-term, clinically benificial effects. Replication of the entrainment effects of MNS in MEG is important to ensure validity of the findings, to investigate whether the effects of MNS are caused by entrainment or SSEPs, and to probe the regional effects of MNS in source rather than sensor space. In MEG the signal is less affected by the conductivity of the overlying tissue compared to EEG (Baillet, 2017; Cheyne, 2013), and therefore the models used for source localisation are simpler due to the lower level of spatial smearing (Muthukumaraswamy, 2014). Furthermore, compared to EEG, MEG has lower susceptibility to interference from non-neuronal sources such as muscles (Boto et al., 2019). Here we hypothesise that there will be entrainment of oscillations within the contralateral somatosensory cortex during rhythmic, but not arrhythmic, MNS. To conclude that rhythmic MNS induces entrainment we will need to show (i) a frequency and region-specific increase in instantaneous amplitude, (ii) synchronisation of the phase with the external source and (iii) that these effects are unlikely to be due to rhythmic evoked potentials. We expect no difference in the online effects of the stimulation at 12 and 20 Hz except for the frequency specificity.

2. Experimental procedures

2.1. Subjects

Twenty healthy participants were recruited for the study. Nineteen participants were right-handed according to the Edinburgh Handedness Inventory (Oldfield, 1971). Participants gave informed consent and the experimental paradigm received local ethics committee approval (School of Psychology, University of Nottingham). Participants agreed that pre-existing structural MRI data (obtained within the Sir Peter Mansfield Imaging Centre, University of Nottingham) could be used by the researchers. One participant (female, 21 years old, right-handed) was excluded prior to analysis due to excessive movement during the MEG recording, leaving 19 usable datasets (aged 26.7 ± 3.6 years (mean ± SD); 11 female). A small inconvenience allowance was provided for volunteers for their participation.

2.2. Median nerve stimulation

Stimulation was delivered with electrodes (cathode proximal) positioned on the right forearm over the median nerve, using a Digitimer constant current stimulator model DS7A (Digitimer Ltd, UK). Pulse width was set at 0.2 ms and maximum compliance voltage (Vmax) was 400 V. Participants were seated and told to rest their forearm on the chair armrest to ensure the muscles were relaxed. The stimulation

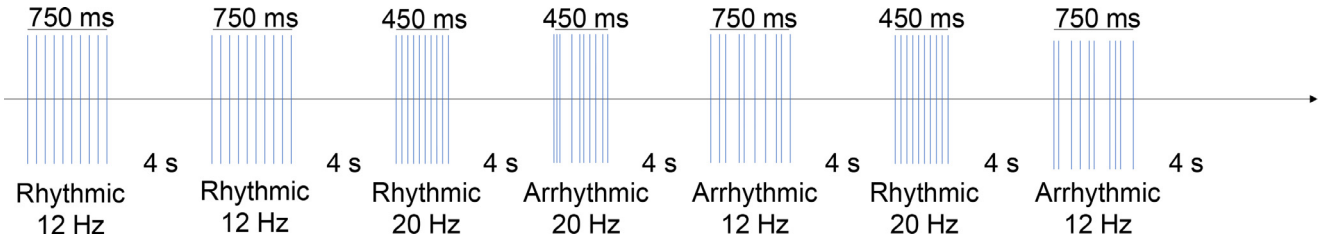

Fig. 1. Stimulation overview. A diagram showing an example of the trial setup for the MNS.

threshold was set at the minimum intensity required for a visible thumb twitch (mean ± SD) 9.1 ± 3.2 mA.

Four hundred trials of stimulation were delivered to the right median nerve during concurrent MEG recording, with a short break every 100 trials. Each trial consisted of 10 pulses delivered at the frequency of interest, rhythmic 12 and 20 Hz in the test conditions. Arrhythmic controls were used to ensure that similar responses did not occur with random stimulation at the same average frequency. During the control trials the same number of pulses were delivered as in the test condition, but with a random inter-stimulus interval (ISI) which was on average the same as the rhythmic trials (but constrained to a minimum ISI of 0.01 s). The arrhythmic patterns were not the same for all trials or participants, however, the first pulse was always delivered at time 0 and the last pulse was always delivered at the end of the train (450 or 750 ms), regardless of the condition. For each of these 4 conditions, 100 trials were randomly delivered with an inter-trial interval of 4 s using an in-house MATLAB script (MATLAB R2012a, Mathworks, Natick, MA) (Fig. 1). The order of the 400 trials was randomised using the Psychtoolbox-3 function 'Shuffle' (Kleiner et al., 2007), and was different for every participant. Of note, here the right median nerve was chosen due to convention in the MNS literature, however we would expect no difference in the results for stimulation of the left median nerve except for the laterality of the effects.

2.3. EMG measurement

To have an objective measure of the contractions caused by MNS, electromyography (EMG) electrodes were placed over the right abductor pollicis brevis (APB) muscle in a belly tendon montage. Motor evoked potentials (MEPs) were recorded for twenty pulses of MNS at the intensity for a minimum thumb twitch, with 3 s between each pulse. A Brainamp ExG (Brain Products GmbH, Gilching, Germany) was used to amplify the signal and Brain Vision Recorder (Brain Products GmbH, Gilching, Germany) was used to record the EMG data (bandpass filtered 10–2000 Hz, sampling rate 5 kHz). Peak-to-peak amplitudes were measured using an in-house MATLAB script to determine the baseline MEP amplitude (mean = 1219.13 μV, range = 52.10 - 7490.9 μV) (MATLAB R2017a, Mathworks, Natick, MA). EMG data from 6 individuals was not recorded due to technical issues.

2.4. MEG data acquisition

MEG data were collected at the Sir Peter Mansfield Imaging Centre, University of Nottingham using a 275-channel CTF MEG system (MISL, Coquitlam, Canada) with participants in a seated position. The system was operated in a third order synthetic gradiometer configuration and data were sampled at 600 Hz. Fiducial marker coils were placed on the nasion and bilateral preauricular points of the participants, to track head movement in relation to the MEG sensors. A Polhemus FASTRAK (Polhemus Inc, Vermont) was used to digitise the participants' head shape and the relative positions of the fiducial markers. The data were examined by eye using commercial MEG data visualisation software (CTF MEG, Canada) and trials containing large artefacts were discarded, as were trials where the head moved more than 7 mm from its initial position. One occipital channel was removed during preprocessing in one subject. Following preprocessing there were on average (mean ± SD) 7 ± 8 rhythmic 20 Hz, 9 ± 10 arrhythmic 20 Hz, 8 ± 9 rhythmic 12 Hz and 8 ± 8 arrhythmic 12 Hz trials removed per subject. The data were then segmented such that an epoch started 1 s before stimulation and ended 3 s following the end of stimulation. The epoch lengths of alpha and beta trials were 4.75 and 4.45 s, respectively. An anatomical MRI scan (1.0 mm^3 resolution, MPRAGE sequence) from each subject was used for co-registration to the digitised head shape.

2.5. Data analysis

After pre-processing, a linear-constraint minimum-variance (LCMV) beamformer was applied to the data (Van Veen et al., 1997). Using FLIRT (FMRIB's Linear Image Registration Tool) (Jenkinson et al., 2012), a MNI (Montreal Neurological Institute) template brain was warped with respect to the subject's downsampled (4 mm) anatomical scan, as was the AAL (Automated Anatomical Labelling) atlas (Tzourio-Mazoyer et al., 2002). This allowed the cortex to be parcellated into 78 regions and the coordinates of the centroids from each region to be determined for each individual (Gong et al., 2009). Covariance was calculated for the entire experimental time window within a 1–150 Hz frequency window (Brookes et al., 2008). The covariance matrix of the filtered data was regularised using the Tikhonov method, with the regularisation parameter set at 5% of the maximum singular value. The forward model was computed using dipole approximation and a multiple local spheres head model (Huang et al., 1999; Sarvas, 1987). Dipoles were rotated in the tangential plane to determine the orientation which yielded the maximum signal-to-noise ratio. Beamformer weights were calculated for the centroid of each brain region resulting in 78 time-courses (O'Neill et al., 2017), which were filtered between 1 and 48 Hz.

2.6. Time frequency spectrograms

To visualise amplitude changes across the trial, time frequency spectrograms were calculated. Data were filtered into overlapping frequency bands spanning from 4 to 50 Hz to visualise the changes across frequency bands in the left somatosensory cortex as defined by the AAL atlas. The analytic signal for the data within each band was determined using a Hilbert transform (HT), the absolute value of which gave the instantaneous amplitude of the MEG signal at each point in time. Time-courses for each frequency band were then averaged across trials, before being normalised using the average amplitude during the control window (0.24–0.99 s for 12 Hz trials and 0.54–0.99 s for 20 Hz trials (length the same as the active time window for that condition)). Time frequency spectrograms were averaged across subjects.

We also calculated the average amplitude during the period of stimulation to investigate the differences between rhythmic and arrhythmic without averaging out the effects of the arrhythmic condition due to the random pulse timings. First the data were filtered into the frequency band of stimulation (11–13 Hz or 19–21 Hz). Then the data from each trial was normalised using the average amplitude during the control window for that trial. Next, we calculated the mean amplitude within the period of stimulation and finally averaged across trials and

subjects. The average amplitude from the periods of rhythmic and arrhythmic stimulation were then compared using a one-tailed Wilcoxon signed rank test.

2.7. Inter-trial phase coherence

The timeseries from the contralateral somatosensory cortex were filtered into the same frequency bands as were previously used for the time frequency spectrogram calculation. Following a HT of the data, the ITPC was calculated using formula (1) below:

$$ITPC = \frac{1}{N}\sum_{k=1}^{N} \exp^{i*}\Phi k \quad (1)$$

Where N is the number of trials and Φk is the phase angle in radians of the datapoint in the current trial.

2.8. Statistical analysis

For both the instantaneous amplitude and ITPC, timecourses were filtered according to the frequency of stimulation (11–13 Hz or 19–21 Hz) using a bandpass least-square linear-phase FIR filter with a filter order of 200. These timecourses were then statistically compared using a one-tailed Wilcoxon signed rank test at each timepoint as the data failed the Kolmogorov-Smirnov test for normality. Multiple comparisons were corrected for using the false discovery rate (FDR) of 0.05 (Benjamini and Hochberg, 1995; Benjamini and Yekutieli, 2001; Groppe, 2020). The same method was used to compare the timecourses following each pulse of rhythmic and arrhythmic stimulation for the evoked potential analysis. Post-hoc timecourse analysis was completed in the same manner but with a two-tailed test. All timecourse plots show the standard error of the mean (SEM) (Martínez-Cagigal, 2020).

2.9. Sensory evoked potentials

Rhythmic sensory evoked potentials would lead to an increase in instantaneous amplitude and ITPC during rhythmic stimulation, providing an alternative mechanism to entrainment (Thut et al., 2011b). To investigate whether this was the case, we looked at whether there was a full oscillation at the frequency of stimulation associated with each pulse of the rhythmic stimulation train to determine whether entrainment had occurred. To do this the beamformed signal was filtered between 11 and 13 Hz for the 12 Hz stimulation trials and 19–21 Hz for the 20 Hz stimulation trials. The data following the pulse timings (83.3 ms for the 12 Hz trials and 50 ms for the 20 Hz trials) were averaged for each of the 10 pulses across all trials for every subject, before being averaged across subjects. The same method was used to look at the broadband (1–48 Hz) signal following each pulse, to investigate whether there was a SEP associated with each MNS pulse. Data from 1 participant were not included in the 20 Hz condition analysis due to a loss of data, meaning we were unable to determine which trials were deleted during preprocessing, and as such could not determine the pulse timings for the remaining trials.

We then took the average broadband (1 – 48 Hz) data from the first pulse of the rhythmic trials and used this as a template SEP for each subject, as this should be equivalent to the SEP seen with a single pulse of MNS. This will have negated the possibility of pulses happening in quick succession in the arrhythmic trials. Using the fitlm MATLAB function (MATLAB R2019a, Mathworks, Natick, MA), we linearly modelled the averaged data for each pulse of the rhythmic and arrhythmic trials in each subject individually using their template SEP. We hypothesised that if the rhythmic response were due to entrainment rather than rhythmic SEPs then the adjusted R-squared value would be significantly higher for the arrhythmic compared to the rhythmic pulses, as the model would explain more of the variance in the response. To compare the fit of the linear model we used a Friedman's two-way ANOVA with rhythmic and arrhythmic as the conditions and pulses for every subject as paired repeats. A non-parametric test was used as the data failed the Kolmogorov-Smirnov test for normality.

To further investigate whether the effects were due to entrainment or rhythmic SEPs, we used empirical mode decomposition (EMD) to decompose the mean trial data for each participant, associated with pulses 3–10 of the rhythmic 12 Hz and 20 Hz stimulation, into intrinsic mode functions (IMFs). Using the EMD python package (Quinn et al., 2021), we computed the IMFs. Then the 'good' oscillatory cycles, with an amplitude above 0.05, were identified. These cycles were then phase aligned and the phase-aligned instantaneous frequency was determined. The phase-aligned instantaneous frequency was calculated for every IMF, for each subject in each condition, and then the IMF with the average instantaneous frequency closest to the frequency of stimulation was selected. Finally, a one-sample *t*-test was performed at every point in the phase cycle to compare the phase-aligned instantaneous frequency from all the good cycles in that IMF to the stimulation frequency. If entrainment had occurred, we would expect a constant instantaneous frequency at the stimulation frequency across instantaneous phase, as is the case with sinusoidal oscillations. Browns method was used to combine the p-values to determine whether there was a significant difference overall for that subject (Poole et al., 2016).

2.10. Individual frequency

The individual alpha and beta frequency for each subject were calculated based on all the conditions together (12 and 20 Hz, rhythmic and arrhythmic), using a 2 s window within the rest period between trials. The MATLAB periodogram function was used to determine which frequency was associated with the maximum power peak within the frequency band of interest. We investigated the relationship between the absolute distance in Hz from the individual frequency and the mean amplitude at the frequency of stimulation using a Spearman's rank test, as the data failed the Kolmogorov-Smirnov test for normality.

3. Results

All analyses were conducted on the contralateral (left) *somatosensory* cortex as defined by the AAL atlas. Results for similar analyses on the contralateral *motor* cortex can be found in the supplementary information.

3.1. Entrainment: increase in instantaneous amplitude

During the delivery of 10 rhythmic pulses at 12 Hz, the source of the increase in oscillatory amplitude at 12 Hz (Fig. 2A) was the contralateral sensorimotor cortex. This increase was not evident during arrhythmic stimulation where a decrease in amplitude was seen bilaterally in the sensorimotor cortices (Fig. 2B). Similarly, during the 20 Hz rhythmic condition the source of the increase in the oscillatory amplitude at 20 Hz (Fig. 2C) was the contralateral sensorimotor cortex, which was not evident during arrhythmic stimulation at the same average frequency (Fig. 2D). Therefore, the rest of our analysis will focus on the contralateral sensorimotor cortex.

Evidence of rhythmic entrainment comes from the time frequency spectrograms where there was an initial broadband increase in amplitude associated with the first pulse (1 s) of both rhythmic (Fig. 3A,D) and arrhythmic stimulation (Fig. 3B,E), which became specific to a narrowband around the frequency of stimulation during only rhythmic stimulation (Fig. 3A,D). This increase in amplitude returned to baseline shortly after the last pulse in the rhythmic condition. When the arrhythmic time frequency spectrogram is subtracted from the rhythmic time frequency spectrogram, it is evident that the difference between trials occurred only during the delivery of stimulation (Fig. 3C,F). The 12 Hz relative amplitude within the window of stimulation was significantly higher in the rhythmic condition compared to arrhythmic ($p \leq 0.05$ between 1093 and 1883 ms, FDR corrected). Similarly, the 20 Hz relative amplitude

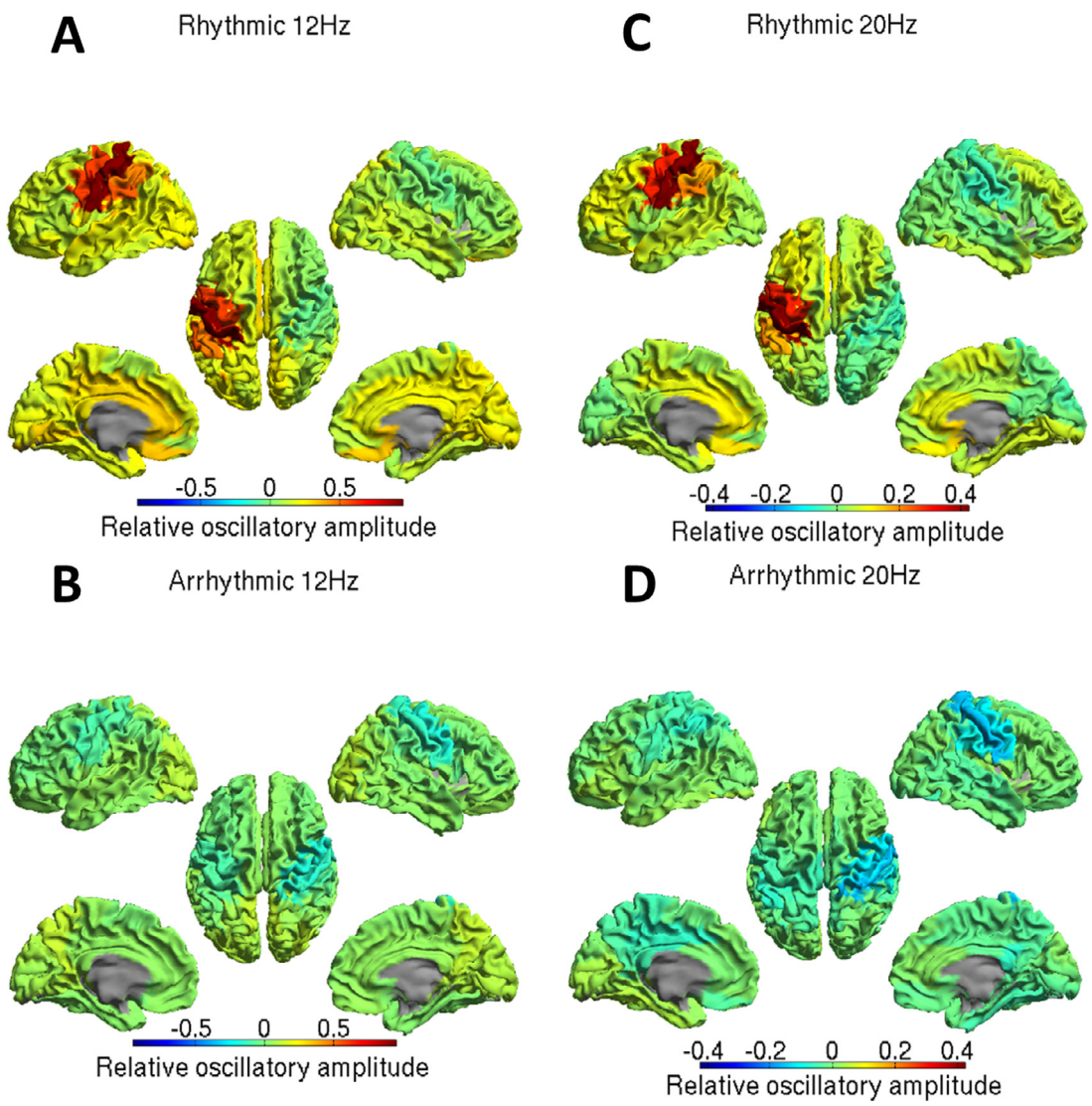

Fig. 2. Localisation of the source of oscillatory changes at the frequency of interest compared to baseline. Oscillatory amplitude for 78 cortical regions of the AAL atlas during (A) rhythmic 12 Hz MNS and (B) arrhythmic 12 Hz MNS, (C) rhythmic 20 Hz MNS and (D) arrhythmic 20 Hz MNS. ($N = 19$, standard deviation of signal during active window (1–1.75 s for 12 Hz trials 1–1.45 s for 20 Hz trials) minus control window (0.24–0.99 s for 12 Hz trials and 0.54–0.99 s for 20 Hz trials)).

significantly increases within the window of stimulation in the rhythmic condition compared to arrhythmic ($p \leq 0.05$ between 1127 and 1557 ms, FDR corrected). As the arrhythmic condition involved pulses being delivered at different times during every trial, amplitude changes may have been averaged out during calculation of the time frequency spectrogram. Therefore, we calculated the average amplitude at the frequency of stimulation during the period that pulses were delivered for each trial before averaging across trials (Fig. 4). This showed a significantly higher 20 Hz amplitude in the rhythmic compared to the arrhythmic condition ($t = 182$, $z = 3.48$, $p < 0.001$). Analysis of the average amplitude across trials in the 12 Hz condition again showed significantly higher 12 Hz amplitude in the rhythmic condition ($t = 189$, $z = 3.76$, $p < 0.001$).

3.2. Entrainment: increase in phase coherence

For both rhythmic and arrhythmic stimulation, there was an initial increase in ITPC across a wide range of frequencies (Fig. 5). After the first stimulation pulse, this increase in ITPC was maintained in only the rhythmic condition and centred on the frequency of stimulation and its harmonics (Fig. 5A,D). The ITPC within the window of stimulation was significantly higher in the rhythmic condition compared to arrhythmic (12 Hz: $p \leq 0.05$ between 1047 and 1990 ms, FDR corrected) (20 Hz: $p < 0.05$ between 960 and 1700 ms and at 1703 ms, FDR corrected).

3.3. Entrainment: hemispheric specificity

To investigate whether the effect was hemisphere specific, as suggested by the results shown in Fig. 2, we analysed the relative amplitude at the frequency of stimulation in the right and left somatosensory cortices during the rhythmic trials. The increase in relative amplitude during the 12 Hz rhythmic stimulation ($p \leq 0.05$ between 1105 and 1842 ms, FDR corrected) and the subsequent rebound ($p \leq 0.05$ for 3715–3960 ms, 4397–4405 ms and at 4417 ms, FDR corrected) was significantly higher in the left somatosensory cortex, which is contralateral to the stimulated arm. Similarly, the increase in amplitude in the left hemisphere during the 20 Hz rhythmic stimulation was significantly higher ($p \leq 0.05$ between 1152 and 1520 ms, FDR corrected), as was the subsequent rebound ($p \leq 0.05$ for 1993–3165 ms, 3168–3173 ms, 3223–3373 ms, 3632–3637 ms, 3643–3867 ms, 3875–3902 and 3968–4092 ms, FDR corrected).

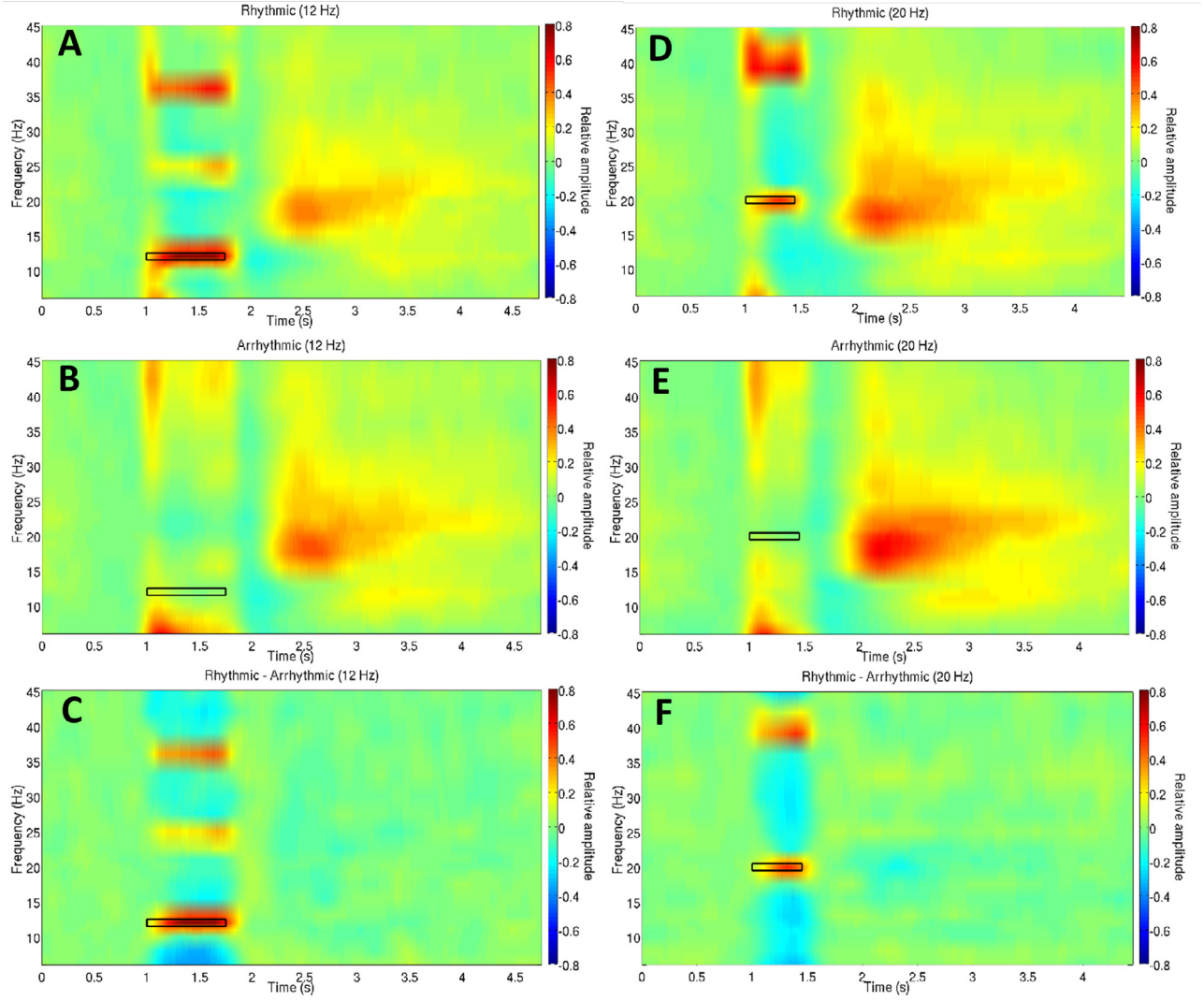

Fig. 3. Relative amplitude in the contralateral somatosensory cortex. (A–C) Time frequency spectrograms of relative amplitude changes when 12 Hz MNS was delivered between 1 and 1.75 s in either a (A) rhythmic or (B) arrhythmic pattern with (C) showing the difference in amplitude between the two conditions. (D–F) Time frequency spectrograms of relative amplitude changes when 20 Hz MNS was delivered between 1 and 1.45 s in a (D) rhythmic (E) arrhythmic pattern with (F) showing the difference in amplitude between the two conditions.

3.4. Sensory evoked potentials

A possible explanation for the increase in instantaneous amplitude and ITPC seen during stimulation is that there was a SEP associated with each pulse of the MNS (Thut et al., 2011b). Therefore, we investigated whether each rhythmic pulse was associated with a full oscillation at the frequency of stimulation and whether this could be explained by the filtering of an SEP (Fig. 6). Each subplot contains the data following the pulse timings in each condition for a complete oscillation at the frequency of stimulation meaning a timeframe of 83.3 ms was used for the 12 Hz trials and 50 ms for the 20 Hz trials. As is evident in the frequency filtered data, a full oscillatory cycle was associated with each pulse of both the rhythmic and arrhythmic trains (Fig. 6A,C). However, this is less clear in the broadband 1–48 Hz data with a SEP being associated with the first pulse of the train (Fig. 6B,D). In Fig. 6A,C the timings were shifted by 20 ms to account for the approximate time it would take for the afferent volley to reach the cortex. The data in Fig. 6B,D were not shifted and the negative deflection at ~20 ms (N20 peak) reflects when the signal arrived in the primary somatosensory cortex (Passmore et al., 2014).

To determine whether these effects were indeed due to entrainment rather than SEPs, we linearly modelled the responses to each pulse in each participant using the SEP associated with the first pulse of rhythmic stimulation as the template. Following the first pulse of stimulation the variability explained by the model decreased for both rhythmic and arrhythmic conditions (Fig. 7). However, the variability explained in the arrhythmic trials was significantly higher than the rhythmic trials (12 Hz: $\chi^2(1) = 80.7$, $p < 0.001$; 20 Hz: $\chi^2(1) = 11.58$, $p < 0.001$). Examples of individual subject fits can be found in the supplementary information.

To further investigate these entrainment effects, we used EMD to decompose our data into IMFs. After selection of our frequency specific IMF, we compared the phase-aligned instantaneous frequency to the stimulation frequency at each phase of the oscillatory cycle. For the 12 Hz rhythmic stimulation 15 out of the 19 subjects did not have an instantaneous frequency that was significantly different to 12 Hz ($p > 0.05$), suggesting entrainment had occurred. For the 20 Hz rhythmic trials, 5 subjects were excluded due to them having fewer than 2 'good' oscillatory cycles. Out of the 13 subjects included in the analysis 10 subjects did not have an instantaneous frequency that was signifi-

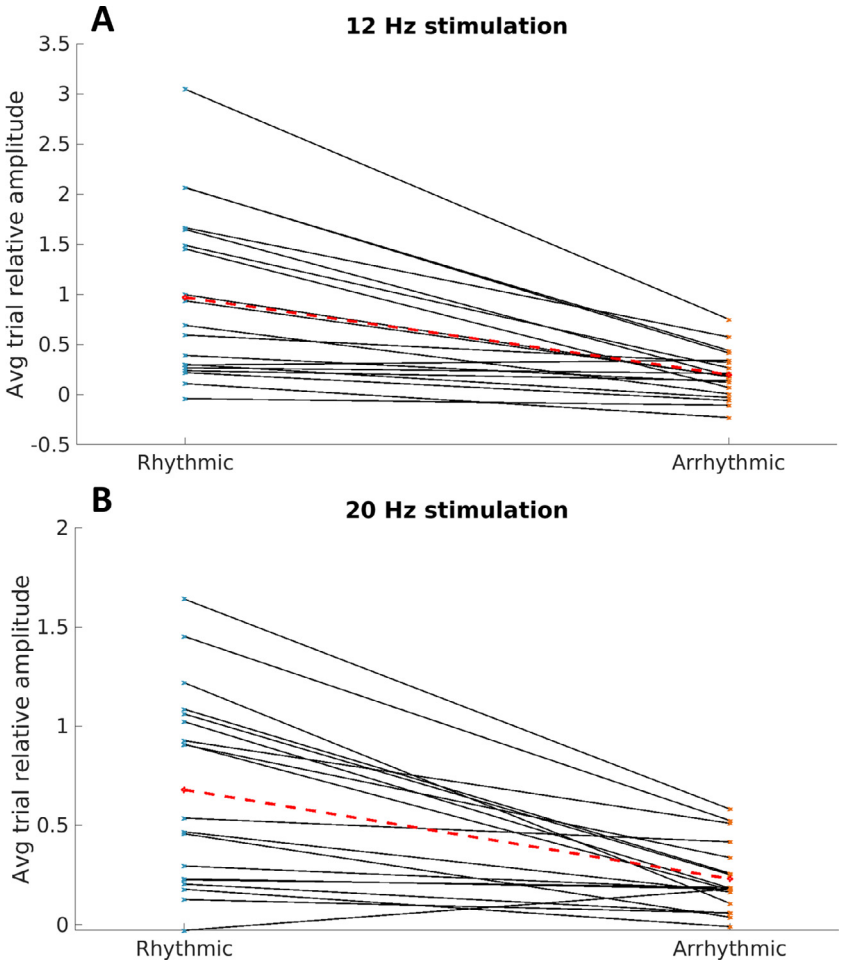

Fig. 4. Intra-subject comparison of average relative amplitude in the contralateral somatosensory cortex. A scatterplot contrasting the average relative amplitude across trials for subjects during rhythmic and arrhythmic patterns of (A) 12 Hz (t = 189, z = 3.76, p = 0.000084) and (B) 20 Hz stimulation (t = 182, z = 3.48, p = 0.00025).

cantly different to 20 Hz ($p > 0.05$), suggesting entrainment occurred for those subjects.

3.5. Post-hoc analyses

Due to the evidence of aftereffects seen in the paper by Morera et al. (2020b), we also investigated the mu-alpha (8–12 Hz) and beta (13–30 Hz) frequency band effects following both 12 and 20 Hz stimulation. The only significant effect was in the mu-alpha (8–12 Hz) band during 20 Hz arrhythmic stimulation compared to rhythmic stimulation, indicating a greater degree of suppression in the rhythmic trials compared with the relative increase in mu-alpha instantaneous amplitude during 20 Hz arrhythmic stimulation as seen in Fig. 3(D–F) ($p \leq 0.05$ for 1123–1353 ms and 1387–1487 ms, FDR corrected). There were no significant differences in the aftereffects of rhythmic and arrhythmic stimulation.

For completeness, we investigated the association between the absolute difference in individual frequencies from the stimulation frequency and the average amplitude at the frequency of stimulation (Fig. 4). Individual frequencies were calculated using 2 s of data from the rest period between stimulation trains from all conditions (rhythmic and arrhythmic, 12 and 20 Hz stimulation). The individual alpha frequency was 9.65 Hz ± 0.31 (mean ± SEM) (range: 8.00 – 12.00 Hz), while the individual beta frequency was 17.73 Hz ± 0.77 (mean ± SEM) (range: 13.00 – 25.20 Hz). There was no significant correlation between the difference from individual alpha frequency and the amplitude at 12 Hz during 12 Hz rhythmic stimulation (r_s=0.1116, p = 0.6492, N = 19) nor the difference from individual beta frequency and the amplitude at 20 Hz during 20 Hz rhythmic stimulation (r_s=−0.0939, p = 0.7021, N = 19).

As the beneficial effects of rhythmic MNS on tics were not restricted to the stimulated limb, as demonstrated in a recent paper by Morera and colleagues, we decided to investigate the spread of the effect using a voxel LCMV beamformer (Morera Maiquez et al., 2020b). This revealed that the source location was in the contralateral sensorimotor hand region (Supplementary information).

4. Discussion

We investigated whether rhythmic MNS could be used to entrain oscillations at frequencies associated with sensorimotor inhibition, mu-alpha (12 Hz) and beta (20 Hz). Our results demonstrate that rhythmic 12 Hz stimulation resulted in an increase in the relative amplitude and ITPC at 12 Hz for the duration of the stimulation in the contralateral somatosensory cortex. Both findings can be split into two segments: (1) an increase in both amplitude and ITPC across a broad range of frequencies for the first pulse in both the rhythmic and arrhythmic trials; (2) an increase specific to the frequency of stimulation for the remainder of the pulse train, which was only seen in the rhythmic condition. We also show that for 12 Hz MNS, a template SEP fit the response to arrhythmic pulses significantly better than the response to rhythmic pulses in individual subjects. These effects were replicated in the 20 Hz condition. These results, and the evidence they provide as to whether MNS can entrain neuronal oscillations, are discussed below.

4.1. Steady-state evoked response

Thut et al. (2011b) previously showed that ~10 Hz TMS caused an initial broadband increase in amplitude in both the rhythmic and ar-

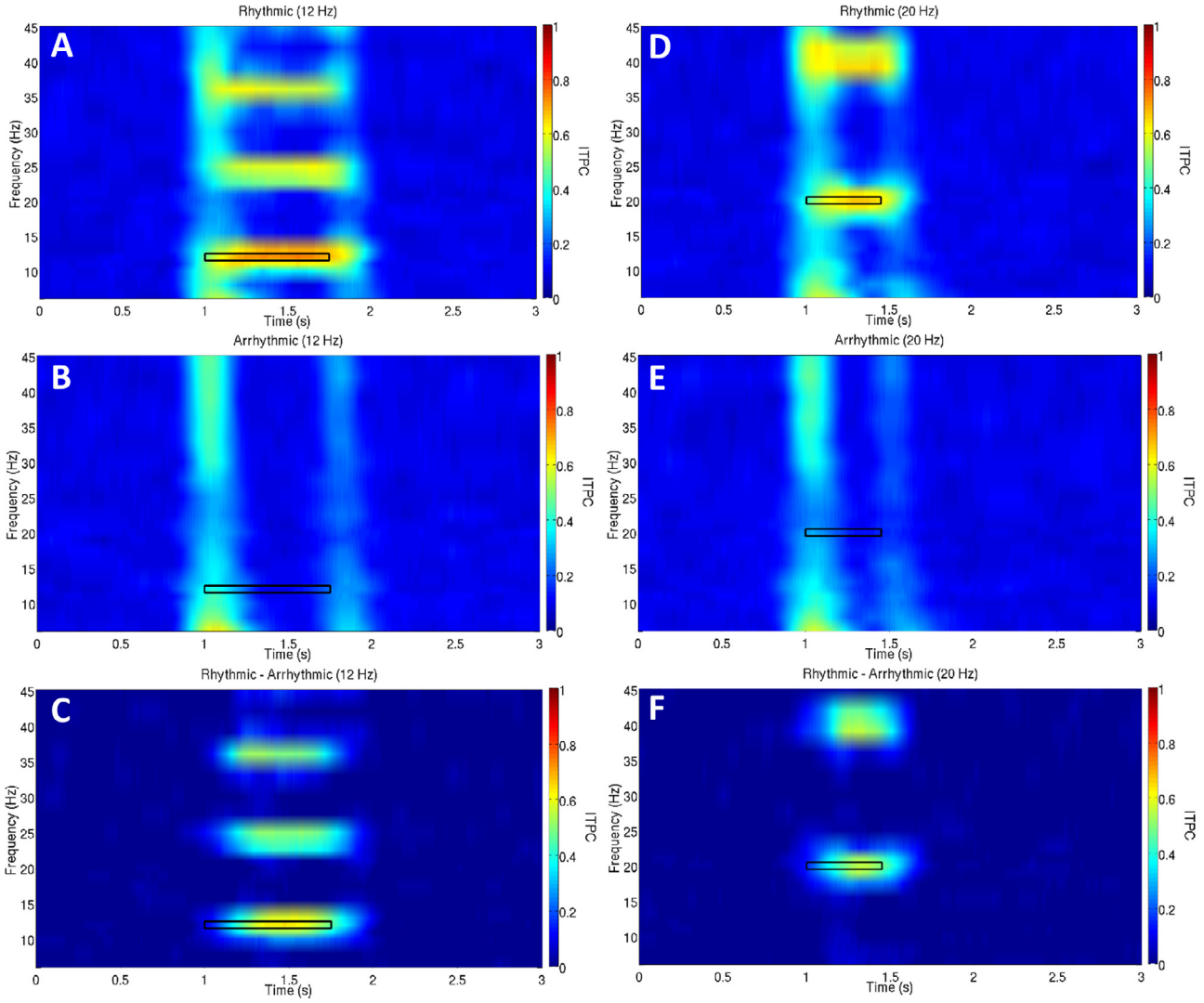

Fig. 5. Inter-trial phase coherence in the contralateral somatosensory cortex. (A–C) Time frequency spectrograms of ITPC when 12 Hz MNS was delivered between 1 and 1.75 s in (A) rhythmic (B) arrhythmic pattern with (C) showing the difference in ITPC between the two conditions. (D–F) Time frequency spectrograms of ITPC when 20 Hz MNS was delivered between 1 and 1.45 s in a (D) rhythmic (E) arrhythmic pattern with (F) showing the difference in ITPC between the two conditions.

rhythmic stimulation conditions, before progressive entrainment was seen in the rhythmic condition. The authors proposed that the delivery of the first few pulses may have resulted in phase resetting of neural generators within the cortex whose frequencies of oscillation varied across a broad range of frequency bands (Thut et al., 2011b). Therefore, phase resetting of these oscillators could have resulted in the initial broadband increase in amplitude. The subsequent pulses however will have only occurred in phase with generators oscillating in the alpha band leading to progressive synchronisation of oscillations at this frequency (Thut et al., 2011b).

Here we show that MNS causes an initial broadband increase in relative amplitude, suggesting that peripheral stimulation triggers an initial phase reset of the neural generators within the contralateral somatosensory cortex regardless of the pattern of stimulation. In line with the theory of entrainment we see that the remainder of the rhythmic pulses cause a frequency specific increase in amplitude. This is also mirrored in the ITPC results, where the initial broadband increase aligns with the theory that numerous neural generators phase reset resulting in phase coherence across trials. As the remaining rhythmic pulses are associated with an increased ITPC in the stimulated frequency band (and its harmonics) this shows that oscillations across trials are relatively more in phase during the stimulation suggesting synchronisation with the pulses of MNS. These findings are consistent with previous reports of a frequency specific increase in EEG power and ITPC during 12 and 19 Hz MNS (Morera Maiquez et al., 2020b; 2020a (preprint)).

However, one central issue in concluding that a rhythmic oscillatory response to a rhythmic stimulus is neural entrainment is whether the same data could be explained by rhythmic evoked potentials (For in-depth review please see Thut et al. 2011a; Zoefel et al. 2018). If we deliver a stimulus at 12 Hz it is expected that we would see a response 12 times a second (Zoefel et al., 2018). An investigation of this possibility by Capilla and colleagues showed that the oscillatory response seen during rhythmic stimulus presentation can be modelled through linear superposition of evoked potentials, which casts doubt on the explanation of entrainment (Capilla et al., 2011). As both responses are expected to repeat at the same frequency, this makes it difficult to determine whether there is underlying entrainment (Zoefel et al., 2018). Furthermore, we would expect oscillations to continue after stimulation if entrainment had taken place (Thut et al., 2011a; Zoefel et al., 2018). During entrainment oscillators become phase-aligned to the external source and, as phase is a free parameter, any change in phase

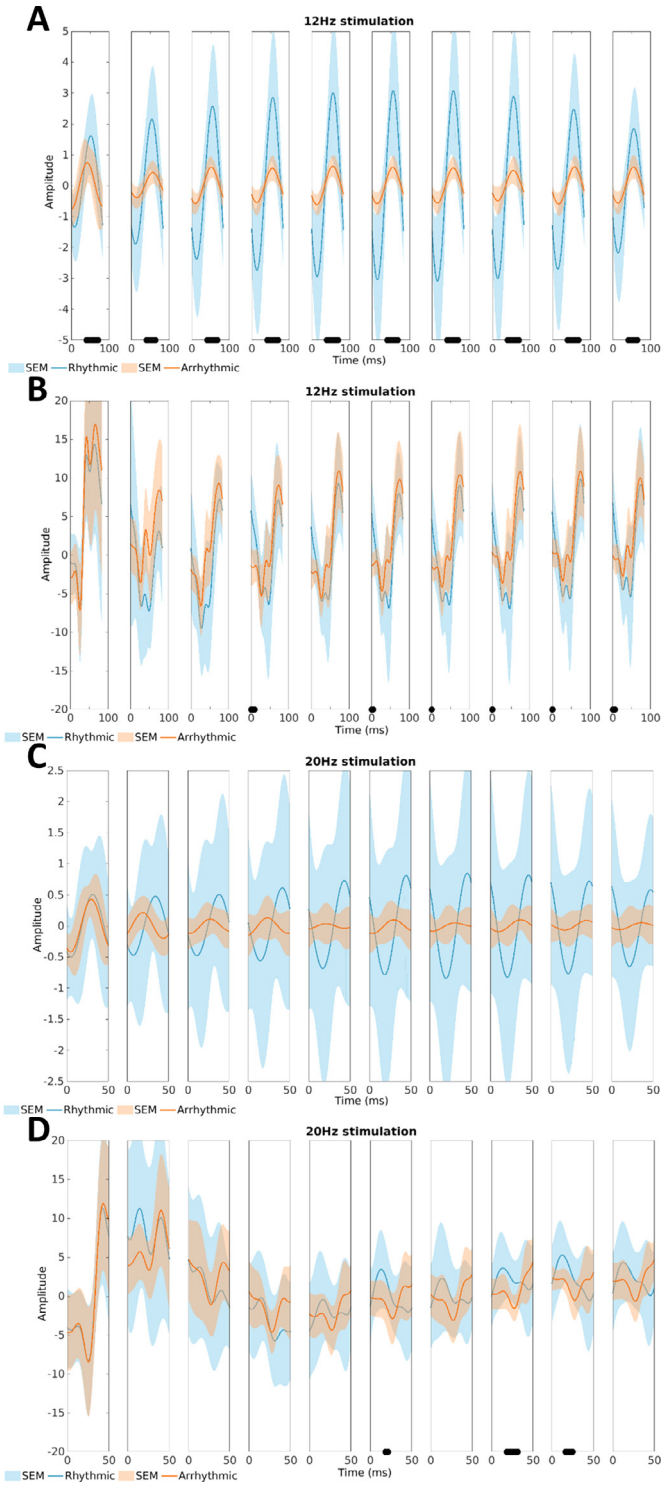

Fig. 6. Evoked components in the contralateral somatosensory cortex. A figure showing: (A) The 12 Hz oscillatory response to each pulse of the rhythmic and arrhythmic 12 Hz MNS. (B) The broadband (1–48 Hz) signal following each pulse of the rhythmic and arrhythmic 12 Hz MNS. (C) The 20 Hz oscillatory response to each pulse of the rhythmic and arrhythmic 20 Hz MNS. (D) The broadband (1–48 Hz) signal following each pulse of the rhythmic and arrhythmic 20 Hz MNS. A black line along the x-axis marks timepoints where a significant difference ($p \leq 0.05$) is seen (FDR corrected).

alignment should only occur if the system is perturbed (Pikovsky et al., 2003). Here, we see a short-lived continuation of the increase in amplitude after the last pulse of MNS, but this could be due to an evoked potential associated with this last pulse.

Fitting a subject specific SEP template to each pulse demonstrated that at the individual subject level the model was significantly better at explaining the variability in the arrhythmic response compared to the rhythmic response. Also, for most subjects the phase-aligned instantaneous frequency of the selected IMF was not significantly different from the stimulation frequency. These results suggest that entrainment occurred. Furthermore, we demonstrated that the difference between the stimulation frequency and the individual frequency was not associated with the amplitude of the response seen at the stimulation frequency. This contrasts with previous evidence that suggests that entrainment is strongest when delivered at the individual's preferred frequency (Romei et al., 2016). Preferred frequencies are usually identified during a separate experiment prior to intervention with NIBS to ensure there are no carryover effects from the stimulation. Therefore, the effect of distance of stimulation frequency from the individual's preferred frequency should be further investigated. The use of 12 Hz here rather than 10 Hz, which is the average alpha frequency, may have made it more difficult to induce entrainment effects, as the oscillatory frequency is more likely to be further from the individual alpha frequency. As 10 Hz MNS would be more tolerable compared with 20 Hz stimulation, the entrainment, and the long-term behavioural effects of this frequency of stimulation should also be explored.

Both evoked potentials and entrained oscillations are generated by synchronous firing of neuronal populations within the contralateral somatosensory cortex meaning these neurons are engaged in processing of the afferent input. As both 12 and 20 Hz stimulation have been shown to slow movement (Joundi et al., 2012; Morera Maiquez et al., 2020b; Pogosyan et al., 2009), we would expect no difference in the online behavioural effects of these stimulation frequencies. Recent research has already demonstrated the possibility that rhythmic 10 Hz MNS could be therapeutically beneficial in reducing tic frequency in Tourette syndrome patients (Morera Maiquez et al., 2020b). It is thought that there is a high level of 'sensorimotor noise' associated with the occurrence of tics in Tourette syndrome leading to a difficulty in discriminating between the signals preceding voluntary and involuntary movement (Ganos et al., 2015). Increasing synchronised firing of neuronal populations within the sensorimotor cortex through MNS may lead to a decrease in this noise. Alternatively, it is known that ~20 ms following median nerve stimulation there is a decrease in the amplitude of MEPs elicited by a TMS pulse to the contralateral motor cortex in a process known as short afferent inhibition (Tokimura et al., 2000). As there is thought to be a deficit in this form of inhibition in Tourette syndrome patients it could be that continuous MNS compensates for this deficit and aids in the inhibition of tics and urges (Morera Maiquez et al., 2020b; Orth et al., 2005; Orth and Rothwell, 2009). It is therefore of interest as to whether arrhythmic stimulation also reduces the frequency of tics i.e., is the beneficial effect due to short afferent inhibition and/or a decrease in sensorimotor noise or is the rhythmicity of the stimulation important (Morera Maiquez et al., 2020b).

4.2. *Aftereffects of rhythmic stimulation*

The observance of a desynchronisation and rebound of sensorimotor oscillations following MNS trains is typical of that seen following one pulse of MNS (Pfurtscheller, 1981). The only significant difference in the effect seen here was a lower relative amplitude in the 8–12 Hz band during 20 Hz rhythmic stimulation compared to arrhythmic. We found no difference in aftereffects. This contrasts with recent findings which indicated that there was greater mu-alpha and beta desynchronization and increased beta rebound following 19 Hz arrhythmic stimulation (Morera Maiquez et al., 2020a (preprint)). On inspection of the data reported by Morera and colleagues, there is a short period of increased mu-alpha suppression towards the end of the stimulus train and for a short time following rhythmic stimulation, similar to what is seen in our data. This suggests that the typical mu-alpha band desynchronization seen during movement is maintained to a degree in the rhythmic

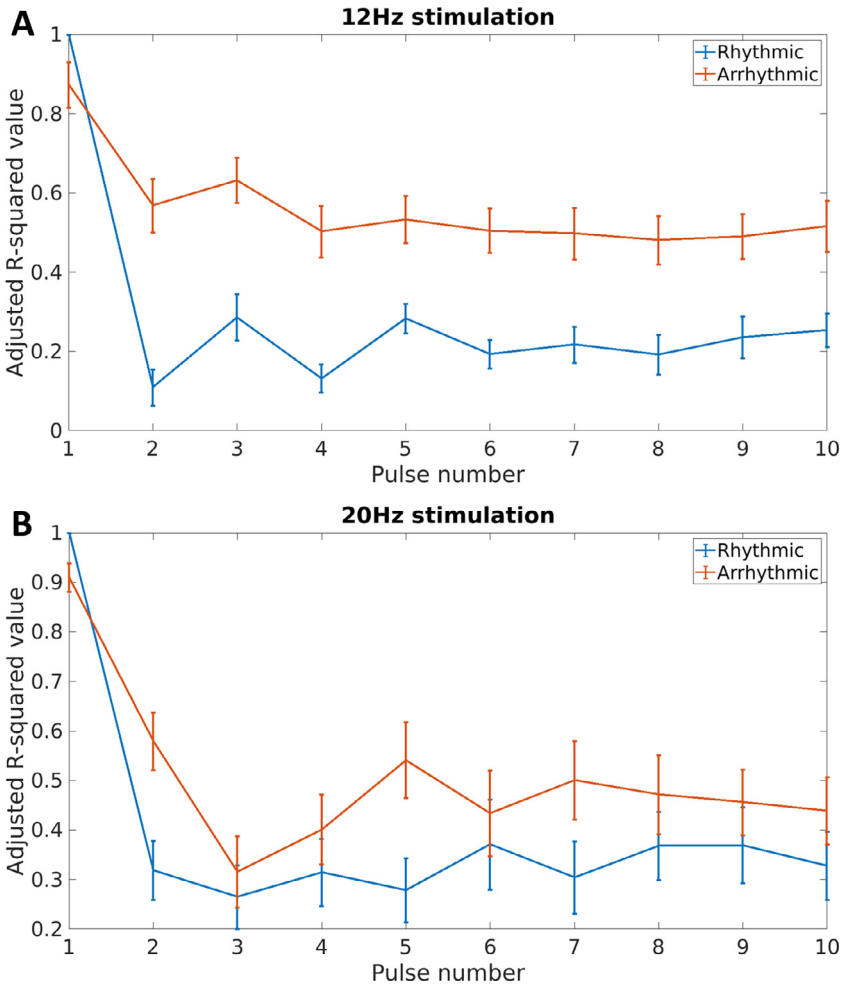

Fig. 7. Model fit when using a subject-specific template sensory evoked potential at each pulse. A figure showing the average adjusted R-squared values for each pulse of (A) 12 Hz and (B) 20 Hz stimulation with error bars showing the SEM.

condition. We hypothesise that the opposite effect of a synchronisation of mu-alpha oscillations during arrhythmic stimulation stems from the stimulation frequency containing components at both lower and higher frequencies to achieve an average frequency of 20 Hz. However, further findings by the same authors also describe greater beta desynchronization and increased beta rebound following 12 Hz arrhythmic stimulation (Morera Maiquez et al., 2020b). A potential factor for the difference in aftereffects seen is the subjective nature of the visible thumb twitch which may have led to participants in one study to experience higher intensities of stimulation. Ultimately further investigation into the aftereffects of rhythmic versus arrhythmic MNS is required. If possible future studies should ideally use an objective method of thresholding, for example, through measurement of MEPs as is common practice with TMS.

5. Conclusion

To conclude, the evidence from this research suggests that endogenous oscillations within the somatosensory cortex can be entrained by 12 and 20 Hz rhythmic MNS. The behavioural effects of rhythmic peripheral nerve stimulation which have been demonstrated by Morera and colleagues are clinically important, however a better understanding of how these behavioural effects are produced is vital for fine-tuning their development as a therapeutic technique (Morera Maiquez et al., 2020b).

Data/code availability statement

- The MATLAB code for MNS delivery is available on OSF https://osf.io/28u6b/
- The MATLAB code for analysis will be made available on OSF https://osf.io/28u6b/
- As the MRI data used during analysis were not collected by the researchers involved, we do not have ethical approval to share these.
- MEG data can be made available on request if a formal data sharing agreement is in place.

Declaration of Competing Interest

The authors declare no competing interests.

Credit authorship contribution statement

Mairi S. Houlgreave: Conceptualization, Methodology, Formal analysis, Data curation, Writing – original draft. **Barbara Morera Maiquez:** Conceptualization, Methodology, Data curation, Writing – review & editing. **Matthew J. Brookes:** Formal analysis, Data curation, Writing – review & editing. **Stephen R. Jackson:** Conceptualization, Methodology, Data curation, Writing – review & editing.

Acknowledgments

This work was supported by a research grant from NIHR Nottingham Biomedical Research Centre and a research grant from the Tourette Association of America. The views expressed are those of the authors and not necessarily those of the NHS, the NIHR or the Department of Health.

Supplementary materials

Supplementary material associated with this article can be found, in the online version, at doi:10.1016/j.neuroimage.2022.118990.

References

Asamoah, B., Khatoun, A., Mc Laughlin, M., 2019. tACS motor system effects can be caused by transcutaneous stimulation of peripheral nerves. Nat. Commun. 10, 1–16 1038/s41467-018-08183-w.

Baillet, S., 2017. Magnetoencephalography for brain electrophysiology and imaging. Nat. Neurosci. doi:10.1038/nn.4504.

Benjamini, Y., Hochberg, Y., 1995. Controlling the false discovery rate: a practical and powerful approach to multiple testing. J. R. Stat. Soc. Ser. B 57, 289–300. doi:10.1111/j.2517-6161.1995.tb02031.x.

Benjamini, Y., Yekutieli, D., 2001. The control of the false discovery rate in multiple testing under dependency. Ann. Stat. 29, 1165–1188. doi:10.1214/aos/1013699998.

Boto, E., Seedat, Z.A., Holmes, N., Leggett, J., Hill, R.M., Roberts, G., Shah, V., Fromhold, T.M., Mullinger, K.J., Tierney, T.M., Barnes, G.R., Bowtell, R., Brookes, M.J., 2019. Wearable neuroimaging: combining and contrasting magnetoencephalography and electroencephalography. Neuroimage 201, 116099. doi:10.1016/j.neuroimage.2019.116099.

Brinkman, L., Stolk, A., Dijkerman, H.C., De Lange, F.P., Toni, I., 2014. Distinct roles for alpha- and beta-band oscillations during mental simulation of goal-directed actions. J. Neurosci. 34, 14783–14792. doi:10.1523/JNEUROSCI.2039-14.2014.

Brinkman, L., Stolk, A., Marshall, T.R., Esterer, S., Sharp, P., Dijkerman, H.C., de Lange, F.P., Toni, I., 2016. Independent causal contributions of alpha- and beta-band oscillations during movement selection. J. Neurosci. 36, 8726–8733. doi:10.1523/JNEUROSCI.0868-16.2016.

Brookes, M.J., Vrba, J., Robinson, S.E., Stevenson, C.M., Peters, A.M., Barnes, G.R., Hillebrand, A., Morris, P.G., 2008. Optimising experimental design for MEG beamformer imaging. Neuroimage 39, 1788–1802. doi:10.1016/j.neuroimage.2007.09.050.

Buchholz, V.N., Jensen, O., Medendorp, W.P., 2014. Different roles of alpha and beta band oscillations in anticipatory sensorimotor gating. Front. Hum. Neurosci. 8, 1–9. doi:10.3389/fnhum.2014.00446.

Capilla, A., Pazo-Alvarez, P., Darriba, A., Campo, P., Gross, J., 2011. Steady-state visual evoked potentials can be explained by temporal superposition of transient event-related responses. PLoS One 6, e14543. doi:10.1371/journal.pone.0014543.

Chen, R., Yaseen, Z., Cohen, L.G., Hallett, M., 1998. Time course of corticospinal excitability in reaction time and self-paced movements. Ann. Neurol. 44, 317–325. doi:10.1002/ana.410440306.

Cheyne, D.O., 2013. MEG studies of sensorimotor rhythms: a review. Exp. Neurol. doi:10.1016/j.expneurol.2012.08.030.

Colon, E., Legrain, V., Mouraux, A., 2012. Steady-state evoked potentials to study the processing of tactile and nociceptive somatosensory input in the human brain. Neurophysiol. Clin. doi:10.1016/j.neucli.2012.05.005.

Engel, A.K., Fries, P., 2010. Beta-band oscillations-signalling the status quo? Curr. Opin. Neurobiol. doi:10.1016/j.conb.2010.02.015.

Ganos, C., Asmuss, L., Bongert, J., Brandt, V., Münchau, A., Haggard, P., 2015. Volitional action as perceptual detection: predictors of conscious intention in adolescents with tic disorders. Cortex 64, 47–54. doi:10.1016/j.cortex.2014.09.016.

Gilbertson, T., Lalo, E., Doyle, L., Di Lazzaro, V., Cioni, B., Brown, P., 2005. Existing motor state is favored at the expense of new movement during 13–35Hz oscillatory synchrony in the human corticospinal system. J. Neurosci. 25, 7771–7779. doi:10.1523/JNEUROSCI.1762-05.2005.

Gong, G., He, Y., Concha, L., Lebel, C., Gross, D.W., Evans, A.C., Beaulieu, C., 2009. Mapping anatomical connectivity patterns of human cerebral cortex using *in vivo* diffusion tensor imaging tractography. Cereb. Cortex 19, 524–536. doi:10.1093/cercor/bhn102.

Groppe, D., 2020. fdr_bh: Benjamini & Hochberg/Yekutieli false discovery rate control procedure for a set of statistical tests [WWW Document]. MATLAB Central File Exchange. URL https://uk.mathworks.com/matlabcentral/fileexchange/27418-fdr_bh (accessed 8.17.20).

Haegens, S., Osipova, D., Oostenveld, R., Jensen, O., 2010. Somatosensory working memory performance in humans depends on both engagement and disengagement of regions in a distributed network. Hum. Brain Mapp. 31, 26–35. doi:10.1002/hbm.20842.

Herrmann, C.S., 2001. Human EEG responses to 1–100Hz flicker: resonance phenomena in visual cortex and their potential correlation to cognitive phenomena. Exp. Brain Res. 137, 346–353. doi:10.1007/s002210100682.

Huang, M.X., Mosher, J.C., Leahy, R.M., 1999. A sensor-weighted overlapping-sphere head model and exhaustive head model comparison for MEG. Phys. Med. Biol. 44, 423–440. doi:10.1088/0031-9155/44/2/010.

Jenkinson, M., Beckmann, C.F., Behrens, T.E.J., Woolrich, M.W., Smith, S.M., 2012. FSL. Neuroimage 62, 782–790. doi:10.1016/j.neuroimage.2011.09.015.

Jenkinson, N., Brown, P., 2011. New insights into the relationship between dopamine, beta oscillations and motor function. Trends Neurosci. doi:10.1016/j.tins.2011.09.003.

Jensen, O., Mazaheri, A., 2010. Shaping functional architecture by oscillatory alpha activity: gating by inhibition. Front. Hum. Neurosci. 4. doi:10.3389/fnhum.2010.00186.

Joundi, R.A., Jenkinson, N., Brittain, J.S., Aziz, T.Z., Brown, P., 2012. Driving oscillatory activity in the human cortex enhances motor performance. Curr. Biol. 22, 403–407. doi:10.1016/j.cub.2012.01.024.

Jurkiewicz, M.T., Gaetz, W.C., Bostan, A.C., Cheyne, D., 2006. Post-movement beta rebound is generated in motor cortex: evidence from neuromagnetic recordings. Neuroimage 32, 1281–1289. doi:10.1016/j.neuroimage.2006.06.005.

Keitel, C., Quigley, C., Ruhnau, P., 2014. Stimulus-driven brain oscillations in the alpha range: entrainment of intrinsic rhythms or frequency-following response? J. Neurosci. doi:10.1523/JNEUROSCI.1904-14.2014.

Kleiner, M., Brainard, D., Pelli, D., Ingling, A., Murray, R., Broussard, C., 2007. What's new in psychtoolbox-3. Perception 36, 1–16.

Martínez-Cagigal, V., 2020. Shaded area error plot. [WWW Document]. MATLAB Central File Exchange. URL https://uk.mathworks.com/matlabcentral/fileexchange/58262-shaded-area-error-bar-plot (accessed 8.17.20).

Morera Maiquez, B., Jackson, G., Jackson, S., 2020a. Entraining movement-related brain oscillations using rhythmic median nerve stimulation. bioRxiv. doi:10.1101/2020.03.30.016097.

Morera Maiquez, B., Sigurdsson, H.P., Dyke, K., Clarke, E., McGrath, P., Pasche, M., Rajendran, A., Jackson, G.M., Jackson, S.R., 2020b. Entraining movement-related brain oscillations to suppress tics in Tourette syndrome. Curr. Biol. 30, 2334–2342e3. doi:10.1016/j.cub.2020.04.044.

Muthukumaraswamy, S.D., 2014. The use of magnetoencephalography in the study of psychopharmacology (pharmaco-MEG). J. Psychopharmacol. doi:10.1177/0269881114536790.

Notbohm, A., Kurths, J., Herrmann, C.S., 2016. Modification of brain oscillations via rhythmic light stimulation provides evidence for entrainment but not for superposition of event-related responses. Front. Hum. Neurosci. 10. doi:10.3389/fnhum.2016.00010.

O'Neill, G.C., Tewarie, P.K., Colclough, G.L., Gascoyne, L.E., Hunt, B.A.E., Morris, P.G., Woolrich, M.W., Brookes, M.J., 2017. Measurement of dynamic task related functional networks using MEG. Neuroimage 146, 667–678. doi:10.1016/j.neuroimage.2016.08.061.

Oldfield, R.C., 1971. The assessment and analysis of handedness: the Edinburgh inventory. Neuropsychologia 9, 97–113. doi:10.1016/0028-3932(71)90067-4.

Orth, M., Amann, B., Robertson, M.M., Rothwell, J.C., 2005. Excitability of motor cortex inhibitory circuits in Tourette syndrome before and after single dose nicotine. Brain 128, 1292–1300. doi:10.1093/brain/awh473.

Orth, M., Rothwell, J.C., 2009. Motor cortex excitability and comorbidity in Gilles de la Tourette syndrome. J. Neurol. Neurosurg. Psychiatry 80, 29–34. doi:10.1136/jnnp.2008.149484.

Passmore, S.R., Murphy, B., Lee, T.D., 2014. The origin, and application of somatosensory evoked potentials as a neurophysiological technique to investigate neuroplasticity. J. Can. Chiropr. Assoc. 58, 170–183.

Pfurtscheller, G., 1981. Central beta rhythm during sensorimotor activities in man. Electroencephalogr. Clin. Neurophysiol. 51, 253–264. doi:10.1016/0013-4694(81)90139-5.

Pfurtscheller, G., Stancák, A., Neuper, C., 1996. Post-movement beta synchronization. A correlate of an idling motor area? Electroencephalogr. Clin. Neurophysiol. 98, 281–293. doi:10.1016/0013-4694(95)00258-8.

Pikovsky, A., Rosenblum, M., Kurths, J., 2003. Synchronization: A Universal Concept in Nonlinear Sciences„ 1st ed. Cambridge Univ. Press, Cambridge.

Pogosyan, A., Gaynor, L.D., Eusebio, A., Brown, P., 2009. Boosting cortical activity at beta-band frequencies slows movement in humans. Curr. Biol. 19, 1637–1641. doi:10.1016/j.cub.2009.07.074.

Poole, W., Gibbs, D.L., Shmulevich, I., Bernard, B., Knijnenburg, T.A., 2016. Combining dependent P-values with an empirical adaptation of Brown's method. Bioinformatics 32 (17), i430–i436. doi:10.1093/bioinformatics/btw438.

Quinn, A., Lopes-dos-Santos, V., Dupret, D., Nobre, A., Woolrich, M., 2021. EMD: empirical mode decomposition and Hilbert-Huang spectral analyses in python. J. Open Source Softw. 6 (59), 2977. doi:10.21105/joss.02977, Vol.Issuep..

Regan, D., 1966. Some characteristics of average steady-state and transient responses evoked by modulated light. Electroencephalogr. Clin. Neurophysiol. 20, 238–248. doi:10.1016/0013-4694(66)90088-5.

Romei, V., Bauer, M., Brooks, J.L., Economides, M., Penny, W., Thut, G., Driver, J., Bestmann, S., 2016. Causal evidence that intrinsic beta-frequency is relevant for enhanced signal propagation in the motor system as shown through rhythmic TMS. Neuroimage 126, 120–130. doi:10.1016/j.neuroimage.2015.11.020.

Sarvas, J., 1987. Basic mathematical and electromagnetic concepts of the biomagnetic inverse problem. Phys. Med. Biol. 32, 11–22. doi:10.1088/0031-9155/32/1/004.

Thut, G., Schyns, P.G., Gross, J., 2011a. Entrainment of perceptually relevant brain oscillations by non-invasive rhythmic stimulation of the human brain. Front. Psychol. doi:10.3389/fpsyg.2011.00170.

Thut, G., Veniero, D., Romei, V., Miniussi, C., Schyns, P., Gross, J., 2011b. Rhythmic TMS causes local entrainment of natural oscillatory signatures. Curr. Biol. 21, 1176–1185. doi:10.1016/j.cub.2011.05.049.

Tokimura, H., Di Lazzaro, V., Tokimura, Y., Oliviero, A., Profice, P., Insola, A., Mazzone, P., Tonali, P., Rothwell, J.C., 2000. Short latency inhibition of human hand motor cortex by somatosensory input from the hand. J. Physiol. 523, 503–513. doi:10.1111/j.1469-7793.2000.t01-1-00503.x.

Tzourio-Mazoyer, N., Landeau, B., Papathanassiou, D., Crivello, F., Etard, O., Delcroix, N., Mazoyer, B., Joliot, M., 2002. Automated anatomical labeling of activations in SPM using a macroscopic anatomical parcellation of the MNI MRI single-subject brain. Neuroimage 15, 273–289. doi:10.1006/nimg.2001.0978.

Van Veen, B.D., Van Drongelen, W., Yuchtman, M., Suzuki, A., 1997. Localization of brain electrical activity via linearly constrained minimum variance spatial filtering. IEEE Trans. Biomed. Eng. 44, 867–880. doi:10.1109/10.623056.

Veniero, D., Vossen, A., Gross, J., Thut, G., 2015. Lasting EEG/MEG aftereffects of rhythmic transcranial brain stimulation: level of control over oscillatory network activity. Front. Cell. Neurosci. 9, 1–17. doi:10.3389/fncel.2015.00477.

Vialatte, F.B., Maurice, M., Dauwels, J., Cichocki, A., 2010. Steady-state visually evoked potentials: focus on essential paradigms and future perspectives. Prog. Neurobiol. doi:10.1016/j.pneurobio.2009.11.005.

Zoefel, B., ten Oever, S., Sack, A.T., 2018. The involvement of endogenous neural oscillations in the processing of rhythmic input: more than a regular repetition of evoked neural responses. Front. Neurosci. doi:10.3389/fnins.2018.00095.